Experimental Neurology 214 (2008) 266–275

Contents lists available at ScienceDirect

Experimental Neurology

journal homepage: www.elsevier.com/locate/yexnr

White matter injury in young and aged rats after intracerebral hemorrhage

Jason K. Wasserman, Lyanne C. Schlichter *

Toronto Western Hospital 399 Bathurst Street, MC 9-415, Toronto, Ontario, Canada M5T 2S8
University Health Network, Canada
Department of Physiology, University of Toronto, Canada

ARTICLE INFO

Article history:
Received 5 July 2008
Revised 6 August 2008
Accepted 16 August 2008
Available online 4 September 2008

Keywords:
Stroke
Traumatic brain injury
Axonal injury
Demyelination
Microglial activation
Amyloid precursor protein

ABSTRACT

Experimental studies of intracerebral hemorrhage (ICH) have focused on neuron death, with little or no information on axonal and myelin damage outside the hematoma. Because development of effective therapies will require an understanding of white matter injury, we examined white matter injury and its spatial and temporal relationship with microglial/macrophage activation in a collagenase model of rat striatal ICH. The hematoma and parenchyma surrounding the hematoma were assessed in young and aged animals at 6 h, 1, 3 and 28 days after ICH onset. Demyelination occurred inside and at the edge of the hematoma; regions where we have shown substantial neuron death. In contrast, there was axonal damage without demyelination at the edge of the hematoma, and by 3 days this damage had spread to the surrounding parenchyma, a region where we have shown there is no neuron death. Because the axonal damage preceded infiltration of activated microglia into the white matter tracts (seen at 3 days), our results support the hypothesis that these cells respond to, rather than perpetrate the damage. Importantly, axonal damage was worse in aged animals, which provides a plausible explanation for the poorer functional recovery of older animals after ICH, despite a similar loss of grey matter. Our findings support strategies that target white matter injury to reduce neurological impairment after ICH.

Introduction

Intracerebral hemorrhage (ICH) is a common and devastating form of stroke. Although the past 10 years have seen substantial progress in understanding the pathogenesis of brain injury (Broderick et al., 2007), no drugs are available to reduce secondary injury and ICH treatment remains primarily supportive (Rincon and Mayer, 2004). One limitation is that almost all preclinical studies have focused on mechanisms of neuron death, while ignoring white matter injury. In 2005, a National Institute of Neurological Disorders and Stroke Workshop on ICH identified white matter injury as a priority for both basic and clinical research. Despite this, no experimental studies have focused on the temporal and spatial progression of white matter injury after ICH.

Damage to either component of white matter – myelin or axons – can disrupt normal neuronal transmission, and both are highly susceptible to hypoxic, excitotoxic and physical insults. Owing to their unusual shape and size, axons are often damaged by mechanical forces after traumatic brain injury (Neumann, 2003). White matter damage is common in acute neurological disorders (traumatic brain injury, ischemic stroke, spinal cord injury) and is considered a key predictor of the outcome (Medana and Esiri, 2003). Both animal and human studies of white matter injury have benefited from immunohistochemistry using antibodies against degraded myelin basic protein to detect demyelination (Matsuo et al., 1997), and amyloid precursor protein to detect axonal damage (Stephenson et al., 1992; Gentleman et al., 1993). Such studies have shown an increase in white matter vulnerability in aged animals (Popa-Wagner et al., 1998; Badan et al., 2004), possibly resulting from enhanced excitotoxicity (Baltan et al., 2008). Two studies using standard histological techniques reported a decrease in the thickness of the corpus callosum at 6 weeks, and a loss of white matter tracts inside the hematoma at 14 weeks after ICH onset (Felberg et al., 2002; MacLellan et al., 2008). However, no studies have assessed acute events resulting in loss of white matter after ICH.

Surprisingly, there is no information on demyelination or axonal damage in the tissue proximal to the ICH hematoma: a region that is characterized by a prominent and prolonged inflammatory response involving activation of resident microglia (Del Bigio et al., 1996; Gong et al., 2000; Wang and Dore, 2007; Wasserman and Schlichter, 2007a). It is intriguing that, despite the ability of activated microglia to kill neurons *in vitro* (Fordyce et al., 2005; Kaushal et al., 2007; Kaushal and Schlichter, 2008), several studies have shown that neuron death does not occur in the parenchyma surrounding the hematoma after ICH (Felberg et al., 2002; Wasserman and Schlichter, 2007a). One possibility is that neuronal somata are relatively resistant and white matter is more vulnerable to inflammatory mediators, such as tumor necrosis factor alpha (TNFα) and nitric oxide (Coleman and Perry, 2002). If so, inflammation after ICH might cause selective white

* Corresponding author. Toronto Western Hospital 399 Bathurst Street, MC 9-415, Toronto, Ontario, Canada M5T 2S8. Fax: +1 416 6035745.
E-mail address: schlicht@uhnres.utoronto.ca (L.C. Schlichter).

0014-4886/$ – see front matter © 2008 Elsevier Inc. All rights reserved.
doi:10.1016/j.expneurol.2008.08.010

matter injury. The present study is apparently the first to focus on the temporal and spatial progression of white matter injury after ICH. Demyelination and axonal damage were assessed from 6 h to 28 days after ICH onset. Of considerable relevance to humans, we also tested the hypothesis that white matter damage is worse in aged animals. Finally, because inflammation has been implicated in white matter injury in other disease models, we assessed the spatial and temporal relationship between microglial activation and damaged white matter tracts.

Materials and methods

Induction of intracerebral hemorrhage

Male Sprague-Dawley rats (n=48; Charles River, Wilmington, MA) were housed in pairs, maintained under a 12 h light/dark cycle, and given food and water *ad libitum*. All procedures were approved by the University Health Network animal care committee, in accordance with guidelines established by the Canadian Council on Animal Care. Young animals were used at 3–4 months. Aged rats (22 months at the time of surgery) were purchased at 12 months and aged in our animal facility.

Intracerebral hemorrhage in the striatum was induced using a method modified from Rosenberg and colleagues (Rosenberg et al., 1990; Wasserman and Schlichter, 2007a). We used less collagenase than before in order to produce a smaller hematoma and avoid ICH-induced mortality in the aged rats. In brief, rats were anesthetized with isofluorane (3% induction, 1.5% maintenance) and placed in a stereotaxic frame. Under aseptic conditions, a 1 mm diameter burr hole was drilled in the skull (0.2 mm anterior and 3 mm lateral to bregma) and a 30-gauge needle was lowered into the right caudate putamen (6 mm ventral to the skull surface). A micropump (Micro4, World Precision Instruments, Sarasota, FL) delivered 0.05 U of bacterial type IV collagenase (Sigma, Oakville, ON) in 0.5 μL saline, at 250 nL/min, after which the needle was left in place for 5 min to prevent solution reflux. Sham-operated animals (n=12) underwent the same surgical procedure and saline injection without collagenase. The core body temperature was maintained at 36.5 °C using an electric heating pad throughout surgery and recovery, and animals regained consciousness within 10 min. Although all animals displayed obvious behavioral deficits within hours of ICH onset (i.e., ipsilateral turning bias), their ability to eat, drink and clean themselves was not impaired. No rats – young or aged – died as a result of surgery or ICH induction.

Tissue preparation

At 6 h, 1, 3 or 28 days after ICH onset, 4–5 animals per group were sacrificed by an overdose of isofluorane, and then perfused through the heart with 100 mL phosphate-buffered saline (PBS), followed by 60 mL of fixative (4% paraformaldehyde, 2% sucrose in PBS; pH 7.5). Dissected brains were stored in the same fixative at 4 °C overnight, followed by 10% sucrose for 24 h and 30% sucrose for 48 h. Fixed brains were cut coronally through the needle entry site, and at 4 mm anterior and 4 mm posterior to that plane. Frozen brain sections (16 μm thick) were made using a cryostat (JungCM 3000, Leica, Richmond Hill, ON) and stored at −80 °C until used. An additional two young rats were sacrificed 3 days after ICH and the brains were treated identically, except that sagittal sections were made through an area of the striatum encompassing the entire hematoma.

Histopathology

Infarcted tissue was visualized by staining brain sections for 10 min in distilled water containing 0.1% cresyl violet. The sections were then briefly immersed in 95% alcohol to improve differentiation. Demyelination and the gross loss of large white matter tracts were visualized using gold chloride, a stain that specifically labels both large myelinated tracts and fine individually myelinated fibers, without labeling neuronal cell bodies (Schmued, 1990). A 0.2% working solution was prepared by dissolving crystalline gold (III) chloride trihydrate (Fisher Scientific Ltd., ON, Canada) in 0.02 M phosphate-buffered saline and stored in the dark at room temperature. Brain sections were incubated in the gold chloride solution at room temperature and monitored until the desired degree of impregnation was achieved (~3 h). Following staining, the slides were fixed in 2.5% sodium thiosulfate for 5 min and then washed in PBS for 10 min. Sections were dehydrated and cover slipped using a non-aqueous mounting medium. An advantage of this stain is that it can be combined with other histological stains, such as Cresyl violet or diaminobenzidine (DAB). The sections can then be viewed at low magnification to assess the spatial relationship between the loss of white matter, neurons and the hematoma.

Hematoma volume

To quantify the volume of the hematoma, frozen brain sections from animals killed 1 day after ICH onset were taken every 200 μm, starting at +2 mm to bregma and extending to −4 mm to bregma. The sections were stained with 3,3'-diaminobenzidine tetrahydrochloride (DAB) containing a metal enhancer (Sigma), which reacts with hemoglobin to form a blue/black stain. Blood-free tissue remains almost clear. Sections were scanned, and the volume of the hematoma was quantified using ImageJ (ver 1.37c, NIH) as: (area of the hematoma in a single section)×(interval between sections; i.e., 200 μm)×(number of sections).

Immunohistochemistry

Single and double labeling and immunofluorescence were performed on 16 μm thick coronal and sagittal sections taken from animals sacrificed at 6 h, 1, 3 or 28 days after ICH onset, as described previously (Wasserman et al., 2007; Wasserman and Schlichter, 2007a). Briefly, sections were incubated (24 h, 4 °C) with the primary antibody in PBS containing 3% donkey serum and 0.3% Triton X-100. After washing in PBS (3×, 5 min each), the sections were incubated (2 h, room temperature) with the secondary antibody in PBS containing 3% donkey serum and 0.3% Triton X-100. The sections were washed again in PBS (3×, 5 min each) and then cover slipped using an aqueous mounting medium consisting of 50/50 glycerol/PBS. Negative controls were treated in the same manner except that the primary antibody was omitted. The following primary antibodies were used: monoclonal mouse anti-MBP (1:50, Chemicon, Temecula, CA) to detect myelin basic protein; polyclonal rabbit anti-APP (1:500, Zymed) to detect amyloid precursor protein; polyclonal rabbit anti-dMBP (1:250, Chemicon) to detect degraded myelin basic protein; polyclonal rabbit anti-Iba1 (1:1000, Wako, Japan) to label microglia. The secondary antibodies were Cy3-conjugated donkey anti-mouse or Alexa 488-conjugated donkey anti-rabbit. Sections were examined using a confocal microscope (Zeiss LSM 510 META, Oberkochen, Germany) and the final images were prepared using ImageJ.

Peri-hemorrhagic amyloid precursor protein and degraded myelin basic protein

To identify regions of myelin damage or demyelination, frozen sections were labeled with an antibody that recognizes degraded myelin basic protein (dMBP), but does not recognize normal MBP in the rat and other species (Matsuo et al., 1997). Amyloid precursor protein (APP) is constitutively produced by neurons throughout the brain and is present throughout their axons. In healthy neurons, its fast anterograde transport maintains a low concentration that is not readily detected by standard immunohistochemical techniques; however, when an axon becomes dysfunctional and protein transport

fails, APP accumulates (Koo et al., 1990; Otsuka et al., 1991; Stephenson et al., 1992; Gentleman et al., 1993; Sherriff et al., 1994). Damaged axons and degraded myelin were monitored at the edge of the hematoma between 6 h and 3 days after ICH onset by staining for APP and dMBP, respectively. For each animal, two brain sections for each marker were taken from an anterior and a posterior location along the length of the hematoma, and staining was quantified in 4 regions of interest (368×368 μm) around the circumference of the hematoma (illustrated in Fig. 1D). One 16 μm serial section was stained with DAB and gold chloride to identify the edge of the hematoma, and then the two polyclonal antibodies (anti-APP and anti-dMBP) were compared in identical regions in a second and third serial section. Confocal images were taken by an observer blinded to the age of the animal, and the amount of APP or dMBP in each image was calculated using ImageJ analysis software with a gray scale threshold, above which all pixels were counted.

Quantification of microglial activation

Pronounced microglial activation occurs in the parenchyma surrounding the hematoma (Del Bigio et al., 1996; Gong et al., 2000; Wang and Dore, 2007; Wasserman and Schlichter, 2007a). To assess whether activated microglia are spatially and temporally associated with damaged axons, white matter tracts in consecutive frozen brain sections were labeled with myelin basic protein (MBP), and then each section was co-labeled with amyloid precursor protein (APP) to mark damaged axons or with 'ionized Ca^{2+} binding protein 1' (Iba1) to label the membranes of microglia/macrophages. To correlate APP+ axons with Iba1+ microglia/macrophages, the same MBP+ white matter tracts were visually identified in the two consecutive serial sections. The same procedure was performed at 6 h, 1 and 3 days after ICH in young and aged animals. There was no need to correlate dMBP+ tracts with microglia because activated microglia were very scarce inside the hematoma until at least 3 days after ICH onset (see Results). Because fully activated microglia can retract their processes, round up and become indistinguishable from macrophages, we use the term microglia/macrophages for these round cells (Streit et al., 1999). Occasionally, a distinction was made wherein microglia were identified as Iba1+ cells with short processes. For each animal, we selected serial sections adjacent to those used above to stain for amyloid precursor protein (APP) and degraded myelin basic protein (dMBP) in each anterior and posterior location along the length of the

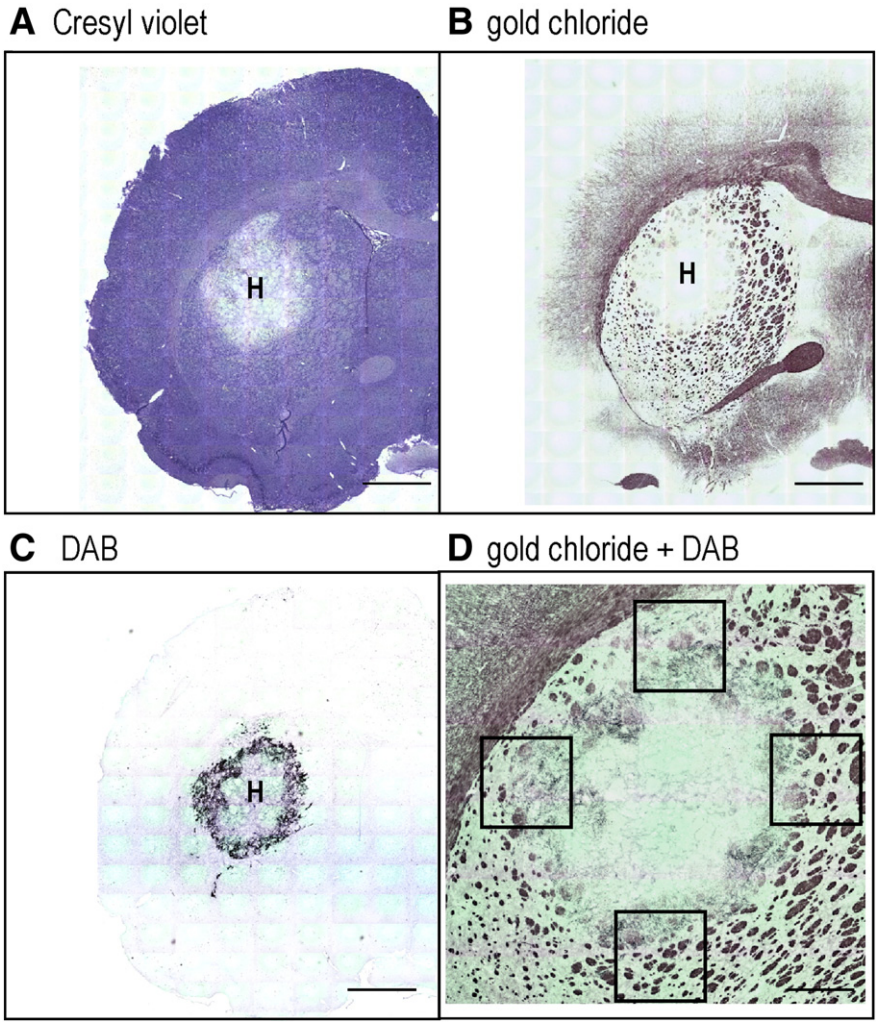

Fig. 1. Spatial relationship between the infarct, white matter loss and the hematoma at 1 day after ICH onset. Each panel represents one of four consecutive 16 μm frozen sections from the same animal. (A) Section labeled with the Nissl stain, Cresyl violet. Lack of Nissl substance, which is found primarily inside neurons, was used to identify the infarct. (B) The white matter stain, gold chloride, shows cross sections of large white matter tracts, which run longitudinally through the normal striatum. Note the loss of Nissl and white matter in the core of the hematoma (H). (C) Staining with 3,3'-diaminobenzidine tetrahydrochloride (DAB), which reacts with peroxidase inside red blood cells. Intact red blood cells at the edge of the hematoma contain more peroxidase and thus appear darker. (D) Fragmented white matter tracts (gold chloride labeled) are present at the edge of the hematoma (DAB labeled), where they are associated with pockets of red blood cells. The boxes show an example of the position and size of regions sampled for cell counting in subsequent figures. Scale bars: 1 mm (A–C); 0.5 mm (D).

hematoma. Then, to quantify activated microglia/macrophages in white matter tracts, the adjacent section was labeled for myelin basic protein (MBP) and Iba1. For each of these sections, four 368×368 μm regions were quantified, which spanned the circumference of the hematoma.

Statistical analyses

Where appropriate, data are expressed as the mean±S.D. for the number of animals indicated. For all statistical analyses, we performed a two-way ANOVA with $p<0.05$ considered significant.

Results

Collagenase injection produced a hemorrhage that was largely restricted to the striatum, with blood only rarely observed in the corpus callosum. By 1 day, the striatal lesion showed little Cresyl violet staining (Fig. 1A), and was essentially devoid of gold chloride labeling (Fig. 1B). DAB staining (Fig. 1C) indicates the hematoma location. These three stains indicate a rapid loss of neurons and white matter throughout the hematoma. The morphology of large tracts further into the parenchyma is like that in the undamaged striatum (not shown). At the edge of the hematoma, fragmented white matter tracts were associated with small patches of blood (Fig. 1D). Before comparing the development of the lesion in young and aged animals, we first assessed whether the extent of bleeding differed between the age groups. At 1 day after ICH onset, the hematoma volumes were not significantly different; i.e., it was 8.7±1.9 mm^3 in young *versus* 9.1±2.6 mm^3 in aged rats ($p>0.1$).

The relationship between demyelination and axonal damage

Staining for degraded myelin basic protein (dMBP; Fig. 2) was especially informative when compared with gold chloride, which stains all myelin in white matter tracts (as in Figs. 1B and D). dMBP staining was prevalent where gold chloride staining was decreased or had a fragmented appearance. In young rats, we found that by 1 day after ICH, many dMBP+ white matter tracts were seen in the core and at the edge of the hematoma, but their morphology was relatively normal (Fig. 2A). However, by 3 days, dMBP staining was lighter and the white matter tracts were more fragmented and larger, consistent with swelling as a result of cytotoxic edema. A similar staining pattern was observed in aged animals. The relative area with damaged MBP (Fig. 2B) significantly increased between 6 h and 1 day in both young and aged animals ($p<0.0001$), and then did not change further by 3 days in either age group. The two age groups did not differ in the extent of dMBP staining at any time examined and, importantly, in the parenchyma outside the hematoma, dMBP was not detected at any of

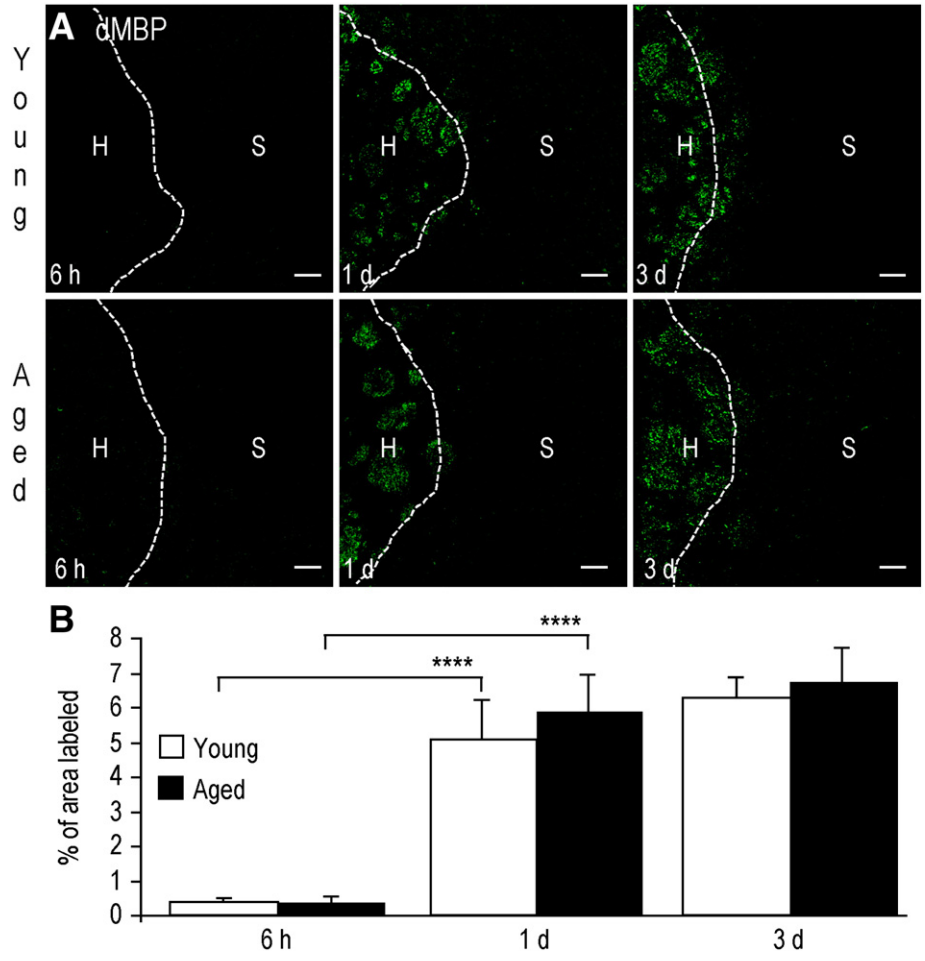

Fig. 2. Damaged myelin in the core and at the edge of the hematoma after ICH. (A) Confocal fluorescence micrographs show damaged myelin, visualized with an antibody against degraded myelin basic protein (dMBP). In both young and aged animals at 1 day after ICH onset, dMBP was observed in the core and at the edge of the hematoma (H), and the dMBP+ tracts retained the structure of normal white matter tracts. By 3 days, the white matter tracts appeared swollen and fragmented. No dMBP was observed in the surrounding striatum (S) at any time examined. The white dotted line shows the edge of the hematoma, as judged by DAB staining in adjacent serial sections. Scale bars: 100 μm. (B) dMBP was quantified in 368×368 μm images by calculating the percentage of the total pixels where the fluorescence level exceeded a threshold that was determined in advance by the ImageJ software. ****$p<0.001$; $n=4$–5 animals per group.

the time points, as is the case in the undamaged contralateral striatum (not shown). At a later time after ICH (28 days), dMBP was not detected in the ipsilateral striatum in either age group, even inside or at the edge of the lesion (not shown).

To identify regions with axon damage (Fig. 3), we used an antibody that recognizes amyloid precursor protein (APP). In both young or aged animals, we observed very little APP staining in the core of the hematoma at any time, but at the edge of the hematoma as early as 6 h there was intense APP staining in large white matter tracts, which ranged from normal morphology to severely fragmented. As time progressed, in both age groups, APP accumulation in white matter tracts extended further into the surrounding parenchyma and the tracts became increasingly fragmented. APP+ white matter tracts were present up to 250 μm from the edge of the hematoma at 1 day after ICH and as far as 400 μm by 3 days. The relative area with APP labeling (Fig. 3B) increased between 6 h and 1 day ($p<0.01$) and increased further between 1 and 3 days in both young and aged animals ($p<0.01$). In aged animals, APP accumulation was greater by 3 days ($p<0.05$). All animals in both age groups had APP outside the hematoma but, interestingly, there was considerable regional variability; APP accumulation was highest in the anterior regions of the caudate nucleus and lowest in the globus pallidus. In both age groups, no APP accumulation was detected outside the hematoma at a later time (28 days; not shown). In young animals at 3 days after ICH, the extent of APP accumulation was evident in sagittal sections; i.e., long APP+ white matter tracts exit the rostral end of the hematoma (Fig. 4A) while, at the caudal end, APP was most concentrated at the edge of the hematoma (Fig. 4B). At higher magnification, end bulbs were frequently observed on transected APP+ axons both rostral (Fig. 4C, arrow) and caudal (Fig. 4D, arrow) to the hematoma. APP+ cell bodies and fragmented axons lined the caudal edge of the hematoma (Fig. 4E, arrow).

We next exploited the ability to identify the same white matter tracts in consecutive frozen sections to examine spatial relationships between three markers of white matter damage in young animals. Serial sections were either labeled with antibodies against myelin basic protein (MBP) plus amyloid precursor protein (APP), or against MBP plus degraded MBP (dMBP). Then, the spatial relationship between APP and dMBP was determined by comparing consecutive sections. At 1 day after ICH, the region of the hematoma corresponded with diffuse MBP staining and lack of morphologically intact MBP+ white matter tracts (Figs. 5A and B). At the same time, APP had accumulated at the edge of the hematoma in fragmented white matter tracts that lacked MBP staining (Fig. 5A, open arrow). There was less APP accumulation in morphologically intact MBP+ tracts in the surrounding parenchyma (Fig. 5A, closed arrow). The

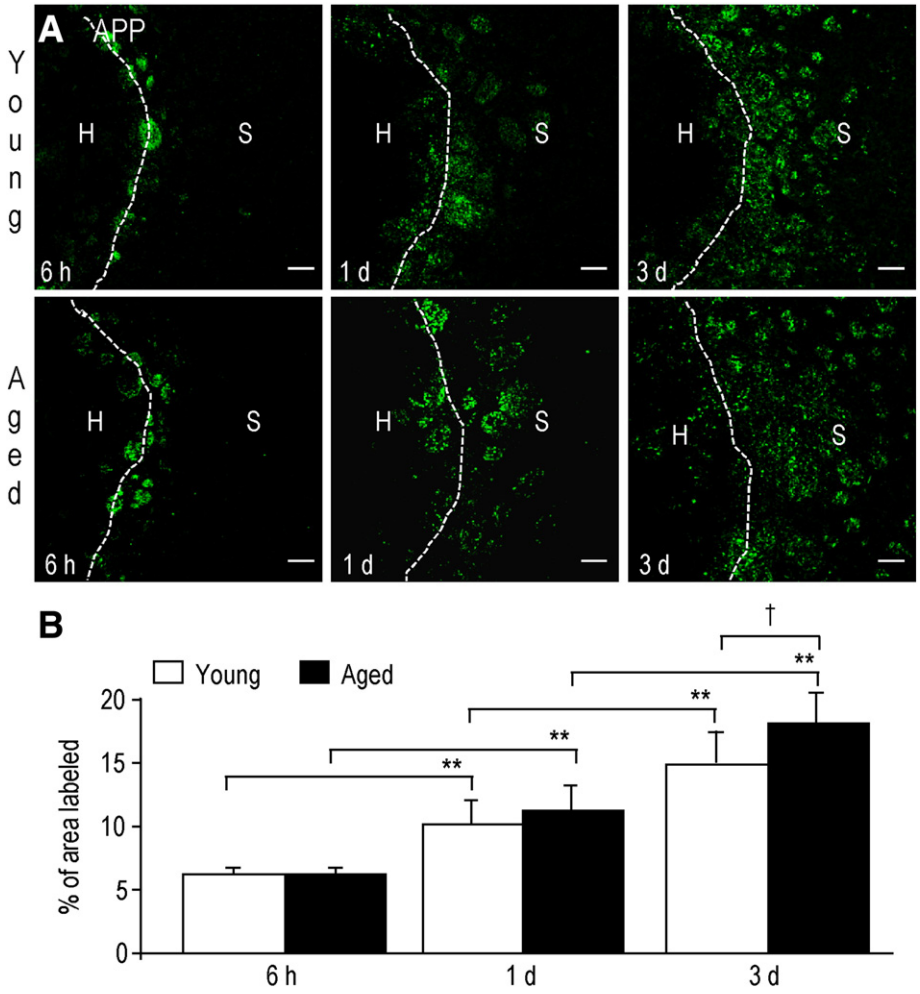

Fig. 3. Damaged axons at the edge of the hematoma and in the surrounding striatum after ICH. (A) Confocal fluorescence micrographs show damaged axons, visualized with an antibody against amyloid precursor protein (APP). In young and aged animals at 6 h after ICH, APP was only observed at the edge of the hematoma (H). At 1 and 3 days after ICH, APP was also observed in the surrounding striatum (S). Note that over time, APP+ white matter tracts of normal morphology were observed further into the surrounding striatum, while those at the edge of the hematoma appeared increasingly fragmented. The white dotted line approximates the edge of the hematoma. Scale bars: 100 μm. (B) APP was quantified in 368×368 μm images by calculating the percentage of the total pixels where the fluorescence level exceeded a threshold that was determined in advance by the ImageJ software. $^{**}p<0.01$; $^{\dagger}p<0.05$ young versus aged; $n=4$–5 animals per group.

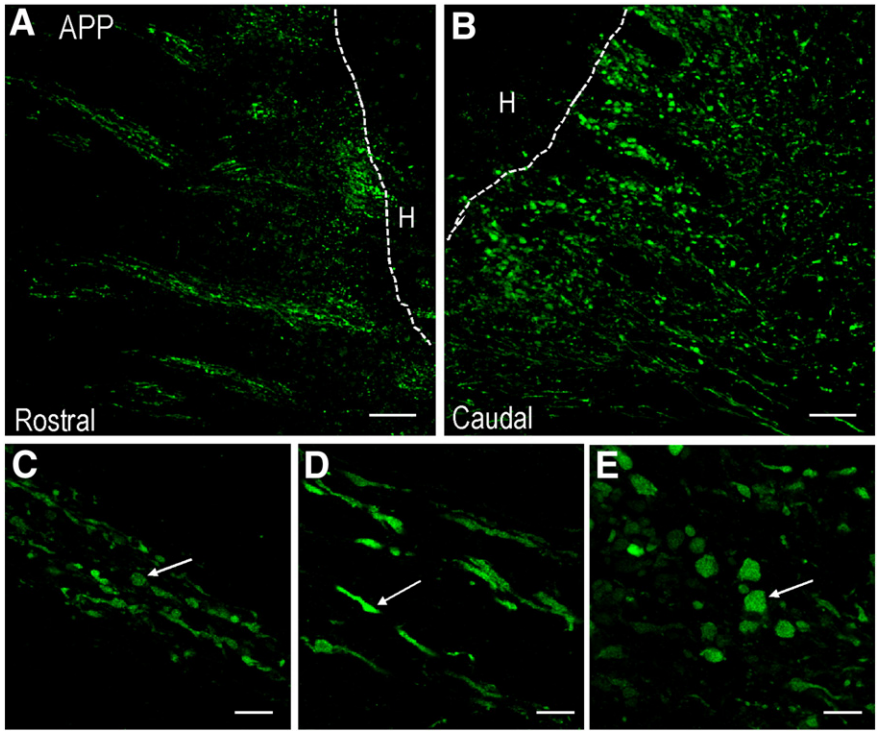

Fig. 4. Sagittal sections show axon damage outside the hematoma at 3 days after ICH onset. Confocal micrographs of sections labeled with antibody against amyloid precursor protein (APP). Lower magnification images show long, APP+ axons in the striatum both rostral (A) and caudal (B) to the hematoma (H). The white dotted line approximates the edge of the hematoma. In the caudal section, APP+ cell bodies and neuropil can be seen. Higher magnification images show APP+ axons (C and D) and cell bodies (E, arrow) outside the hematoma. Note the swollen end bulbs and transected processes (arrows in C and D). Scale bars: 100 μm (A and B); 20 μm (C–E).

ability of the dMBP antibody to selectively label degraded myelin is illustrated by its presence only in areas of white matter that were not labeled with MBP; e.g., in the hematoma (Fig. 5B, open arrow). The non-overlapping distribution of dMBP and MBP staining suggests that as the injury progresses, MBP within affected oligodendrocytes and myelin sheaths becomes degraded and prevents binding of both anti-MBP and dMBP antibodies. Labeling with both APP and dMBP was only observed in white matter tracts at the edge of the

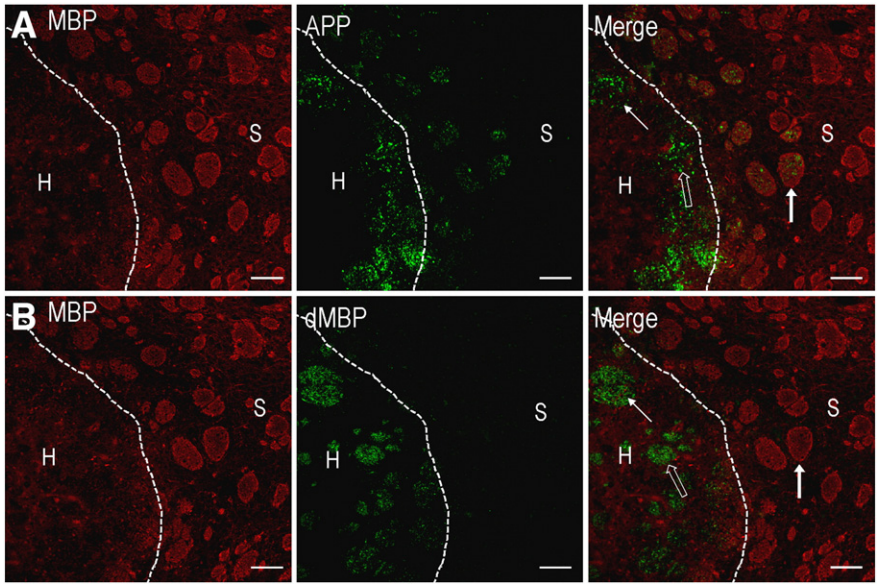

Fig. 5. Spatial relationship between myelin and axonal damage at 1 day after ICH onset. Confocal fluorescence micrographs from serial 16 μm sections. NB: white matter tracts running longitudinally through the striatum were used to view the same tracts in serial sections. This was crucial for showing the relationship between APP and damaged MBP (dMBP) because the two rabbit polyclonal antibodies could not be combined. (A) The section was double labeled for myelin basic protein (MBP) and amyloid precursor protein (APP). APP (open arrow) was observed at the edge of the hematoma (H) and in MBP+ white matter tracts (thick arrow) in the surrounding striatum (S). (B) The section was double labeled for MBP and damaged MBP. dMBP was only observed in the core and at the edge of the hematoma. Note the loss of MBP inside the hematoma, and dMBP labeling of white matter tracts that were not labeled with MBP (open arrow). Thin arrows in A and B show labeling with both APP and dMBP in white matter tracts at the edge of the hematoma. APP (but not dMBP) was observed in normal appearing white matter tracts in the surrounding striatum (thick arrows in A and B). The white dotted line approximates the edge of the hematoma. Scale bars: 100 μm.

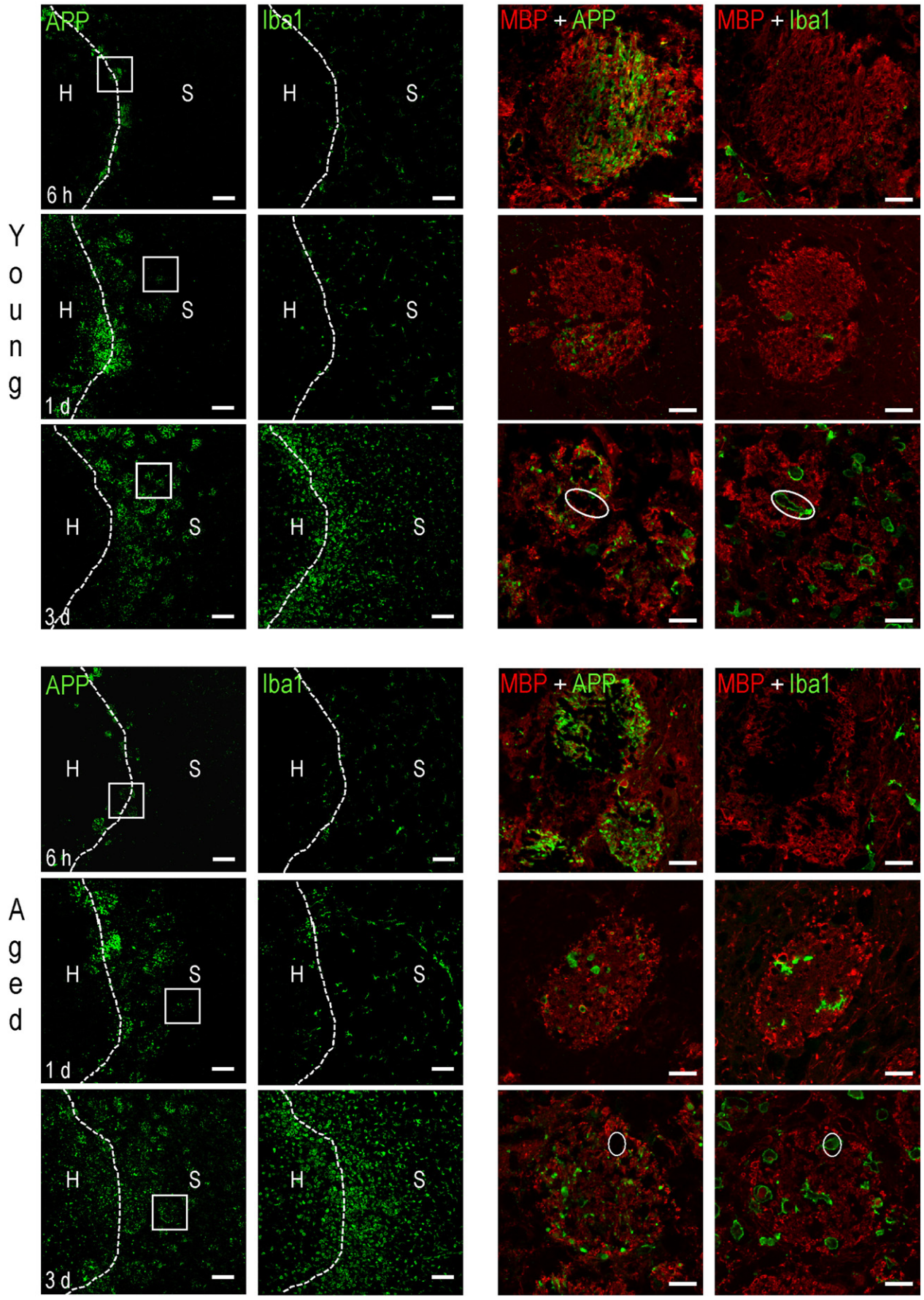
APP
Iba1
MBP + APP
MBP + Iba1
H
S
6 h
1 d
3 d
Young
Aged

hematoma (Figs. 5A and B, thin arrows); whereas, APP+ white matter tracts in the surrounding parenchyma lacked dMBP staining at 1 day (Figs. 5A and B, closed arrows) and 3 days (not shown). Together, these results point to combined axonal damage and demyelination at the edge of the hematoma, but axonal damage without demyelination in the surrounding parenchyma.

The relationship between axonal damage and inflammation

In both age groups, despite accumulation of amyloid precursor protein (APP) and a substantial number of activated microglia at the edge of the hematoma as early as 6 h (see left panels at lower magnification), no activated microglia were observed inside APP+ white matter tracts (see right panels at higher magnification). However, by 1 day, occasional activated microglia/macrophages were detected inside APP+ white matter tracts in the surrounding parenchyma (compare left and right panels). When present, activated microglia/macrophages inside MBP+ white matter tracts were usually close to sites of APP staining at 1 day; this was especially clear for the larger microglia/macrophages of aged animals. Nevertheless, many APP+ tracts did not contain activated microglia/macrophages. In contrast, in both age groups at 3 days after ICH all APP+ tracts appeared fragmented and contained numerous activated microglia/macrophages. Of note, activated microglia/macrophages were often observed inside MBP− white matter 'holes' (examples marked with white ovals in Fig. 6) and they often contained MBP. In morphologically normal APP− white matter tracts, activated microglia with short processes were seen but round microglia/macrophages were absent (not shown). At 3 days after ICH onset, the number of activated microglia/macrophages in MBP+ white matter tracts was significantly higher in aged than in young animals ($p<0.05$; Fig. 7). These observations contrast with the control striatum of naïve animals or the uninjured contralateral striatum of both age groups, where only a few ramified microglia were present in large white matter tracts (not shown).

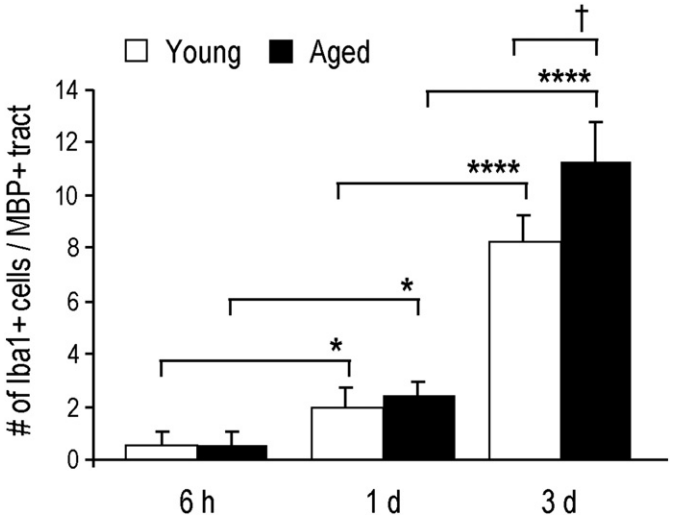

Fig. 7. The number of activated microglia/macrophages within white matter tracts increases with time after ICH and is greater in aged animals. Activated Iba1+ microglia/macrophages were counted inside white matter tracts (MBP) and expressed as the number per white matter tract. Cells were counted in 368×368 μm images encompassing the edge of the hematoma and the surrounding striatum. *$p<0.05$, ****$p<0.001$; †$p<0.05$ young versus aged; $n=4$–5 for each group.

Discussion

This study employed histological and immunohistological methods to characterize the spatial and temporal progression of white matter injury after an intracerebral hemorrhage (ICH) in the anterior striatum (putamen+ caudate) of Sprague–Dawley rats. Surprisingly, this is the first demonstration of demyelination and axonal damage in peri-hemorrhagic tissue after experimental ICH. Because the outcome of ICH is worse in the aged (Gong et al., 2004), we tested the hypothesis that differences in white matter damage might be a contributory mechanism. Our results show that axonal damage in the parenchyma outside the hematoma increased for the first 3 days and was worse in the aged, despite our previous demonstration that no neuron death occurs in this region. In contrast, in both age groups, at the edge of the hematoma (i.e., the zone where we have identified dying neuron cell bodies) there was axonal damage with frank demyelination. Thus, demyelination correlates with neuron cell body damage, not with axonal damage. Next, we asked whether the white matter damage might be mediated by inflammatory cells. Our results support the hypothesis that damage to the axons can occur without demyelination, and that the prominent microglial/macrophage response is not the cause of this axonal damage. That is, in both age groups, most of the axon damage preceded infiltration of inflammatory cells into affected white matter tracts.

Within 1 day of ICH onset, all white matter tracts and neurons inside the hematoma were lost in both age groups. The parenchyma adjacent to the hematoma was more interesting, with fragmented white matter tracts (gold chloride stain) associated with scattered but intact red blood cells (DAB stained). This is consistent with the hypothesis that white matter injury follows contact with blood components that diffuse out of the hematoma in the hours after ICH onset. We further characterized degradation of large white matter tracts by labeling myelin basic protein in both its normal (MBP) and degraded forms (dMBP) in young rats. As with gold chloride, essentially all MBP staining was lost inside the hematoma and, at the edge of the hematoma, many large MBP− tracts also labeled with dMBP. Fragmented white matter tracts adjacent to the hematoma contained both MBP and dMBP, showing that tracts outside the hematoma are progressively damaged for several days after ICH onset.

Amyloid precursor protein (APP) has been used as a sensitive marker of axon dysfunction and damage after other forms of brain injury in animal models and in humans (Stephenson et al., 1992; Gentleman et al., 1993; Sherriff et al., 1994). After traumatic brain injury, APP accumulation demonstrates axon damage as early as 1–3 h and persisting for up to 1 month (Medana and Esiri, 2003). Following ischemic stroke in rats, APP has been observed at the edge, but not in the core of the infarcted tissue (Yam et al., 1997). Consistent with that report, we did not observe APP at any time inside the hematoma in either age group. Instead, a band of APP+ white matter tracts appeared at the edge of the hematoma as early as 6 h after ICH. Together with the pattern of dMBP staining, these results suggest that axons inside the hematoma are lost before APP can accumulate. In contrast, it

Fig. 6. Spatial and temporal relationships between damaged axons and activated microglia/macrophages after ICH. Confocal fluorescence micrographs from serial 16 μm sections at 6 h, 1 day and 3 days after ICH onset. Sections were labeled with antibodies against: amyloid precursor protein (APP) to indicate damaged axons; 'ionized Ca^{2+} binding protein 1′ (Iba1) to label the membranes of activated microglia/macrophages; and myelin basic protein (MBP) to label white matter tracts. Left panels: Lower magnification images of serial sections showing APP and Iba1+ cells at the edge of the hematoma (H) and in the surrounding striatum (S). Because APP and Iba1 were both labeled with rabbit polyclonal antibodies, they could not be combined. Instead, the location of MBP staining was used to spatially correlate APP and Iba1 staining in adjacent serial sections. The white dotted line approximates the edge of the hematoma. Right panels: Higher magnification images of the areas within the white boxes in the left panels. Note that the same MBP+ white matter tracts are identifiable in the two adjacent 16 μm serial sections. The magnified images at 1 and 3 days show the spatial relationship between early APP accumulation and activated microglia/macrophages in the surrounding parenchyma. The white ovals in the 3 day panels show two 'holes' that lack MBP staining but contain an activated microglia/macrophage. Scale bars: 100 μm (left panels); 20 μm (right panels).

appears that white matter injury at the edge of the hematoma is much slower and that protein transport continues for some time after ICH onset. Because accumulation of APP can occur with both irreversible and reversible axonal damage (Stone et al., 2004), we examined other morphological features. Consistent with reports in other types of brain injury (Stephenson et al., 1992; Gentleman et al., 1993; Stone et al., 2004), we observed swollen APP+ axons and end bulbs, and transected axons at both the rostral and caudal edges of the hematoma in young rats. Hence, many APP+ axons were irreversibly damaged. The presence of many APP+ neuronal cell bodies at the caudal edge of the hematoma also demonstrates APP accumulation in neurons whose axons were damaged/transected very close to the cell body. Despite being outside the hematoma, these neurons with transected axons are expected to die soon after ICH.

White matter injury, involving both axons and myelin-producing oligodendrocytes, occurs after a variety of neurological insults. Owing to their large size, unusual shape and relatively high metabolic activity, axons are thought to be particularly susceptible to mechanical injury, transport defects, ischemia and oxidative damage (Neumann, 2003). In some disorders, such as multiple sclerosis, demyelination and axon damage occur at the same time (Marik et al., 2007); whereas, after ischemic stroke and trauma, axon damage occurs in the absence of demyelination (Yam et al., 1997; Medana and Esiri, 2003). In the parenchyma surrounding the hematoma, in both age groups, we observed axon damage (APP accumulation) as early as 1 day after ICH, while demyelination (dMBP staining or loss of MBP) was not observed at any times examined. Myelin damage was restricted to the edge of the hematoma, even at days 1 and 3 when the proportion of large white matter tracts containing damaged axons increased and extended further into the surrounding parenchyma. This observation is crucial because we and others have shown that neuron death is restricted to the edge of the hematoma (Felberg et al., 2002; Wasserman and Schlichter, 2007a), and it supports the view that axons are uniquely sensitive to conditions in the surrounding parenchyma. Furthermore, the failure to detect APP, a sensitive marker of early axon dysfunction, in the surrounding parenchyma until at least 1 day after ICH suggests that a substantial window exists for therapeutic intervention.

As the first investigation of spatial and temporal development of white matter damage in an animal model of ICH, this study necessarily had some constraints. While there are two prevalent rodent ICH models (injection of collagenase or autologous blood) for several reasons, we used stereotaxic injection of Type IV collagenase (Rosenberg et al., 1990; Del Bigio et al., 1996; Wasserman et al., 2007; Wasserman and Schlichter, 2007a; Wasserman and Schlichter, 2007b; MacLellan et al., 2008). Primarily, because our goal was to assess changes in the striatal tissue surrounding the hematoma, we required more consistent lesion volumes and blood locations, which are afforded by the collagenase model (MacLellan et al., 2008). We used a smaller lesion than most previous studies, in order to avoid mortality of aged animals, to prevent bleeding into the ventricles, white matter tracts or cortex, and to allow comparison of perihematomal tissue with the relatively undamaged surrounding striatum. White matter injury outside the hematoma might contribute to lesion growth over time. If so, a larger initial hematoma, with increased mass effect and more blood diffusing into the surrounding parenchyma might worsen the white matter damage and time-dependent increase in lesion size. This possibility further highlights the need to assess white matter damage after ICH. Owing to the small lesion size, behavioral deficits were not assessed because even with much larger striatal hemorrhages, a complicated battery of tests is required to analyze deficits in Sprague–Dawley rats (MacLellan et al., 2006). The most important objective was to analyze the spatial and temporal development of white matter damage in relation to inflammatory cells; thus, we addressed processes and mechanisms that were amenable to immunohistochemical analysis.

Some mechanistic inferences can be made, allowing future studies to address potential molecular mechanisms leading to the white matter injury. From our results, it appears that axons in the tissue surrounding the hematoma are particularly sensitive to damage during the first 72 h after ICH onset. Thus, future studies and therapeutic approaches will need to address the unknown factors that damage axons in the absence of neuronal cell death or demyelination. Within, and at the edge of the hematoma, it is likely that the rapid loss of myelin and axons that we observed results from their being trapped in pockets of blood and exposed to thrombin, complement and products of hemoglobin degradation, especially as all fragmented white matter tracts were associated with red blood cells. Blood-borne neutrophils also accumulate at the edge of the hematoma within 1 day (Del Bigio et al., 1996; Gong et al., 2000; Wasserman and Schlichter, 2007a), where they have the potential to damage white matter through their production of tumor necrosis factor-α, reactive oxygen species and matrix metalloproteases (Redford et al., 1997; Justicia et al., 2003; Nguyen et al., 2007; Wasserman and Schlichter, 2007b). The hypothesis that axons in the surrounding parenchyma are damaged by plasma proteins diffusing out of the hematoma is supported by studies showing that injection of plasma into the brain causes oxidative stress, pro-inflammatory gene expression and DNA damage in nearby white matter (Wagner et al., 2005). Edema, which peaks at 2–3 days as a result of BBB disruption and loss of microvessel integrity in the parenchyma surrounding the hematoma (Xi et al., 2001; Huang et al., 2002; Wasserman and Schlichter, 2007b) should allow additional plasma proteins to enter the brain over a time course consistent with the APP increase in the surrounding parenchyma.

In principle, microglial activation could either cause or result from white matter injury; however, the present results showing that activated microglia/macrophages infiltrate white matter tracts after axonal damage, suggest that they respond to, rather than initiate the damage. There were very few activated microglia/macrophages inside APP+ white matter tracts at 6 h or 1 day, and their numbers did not increase substantially until 3 days. At this later time, affected axons were transected, which is one means whereby activated microglia/macrophages could transform reversible axonal injury into irreversible injury. Regarding grey matter damage, we previously showed that activated microglia/macrophages accumulated at the edge of the hematoma only after neuron death was complete, and their death was neither temporally nor spatially correlated with microglial activation in the surrounding parenchyma (Wasserman and Schlichter, 2007a). This is consistent with studies of ischemic stroke and brain trauma, where microglial activation follows neuronal injury (Morioka et al., 1993; Engel et al., 2000). This temporal sequence has promoted the view that microglia migrate to damaged sites only to remove cellular debris and provide trophic support for regeneration, and this might well be their main role in white matter tracts after ICH. In this aspect, acute CNS damage may differ from some neurodegenerative diseases (e.g., multiple sclerosis), where microglial activation can occur before axon damage or demyelination (Marik et al., 2007).

This work has broader implications. The striatum of both rats and humans is primarily involved in motor and associative functions. It is densely innervated by the cortex, thalamus and substantia nigra pars compacta, and sends most of its projections to the substantia nigra pars reticulata and external portion of the globus pallidus (Tepper et al., 2007). The delayed white matter injury we observed after ICH will prevent neuron contacts with their targets and produce dysfunction of distal structures throughout the brain. Such de-innervation could explain the loss of neurons and decrease in cortical thickness seen in the substantia nigra after striatal ICH (Felberg et al., 2002; MacLellan et al., 2008); hence, future studies should examine loss of neurons in other areas of the brain (i.e., the thalamus) that project extensively into the striatum. Although aging worsens the functional outcome after striatal ICH (Gong et al., 2004), aging did not increase the loss of striatal neurons in the rat model (Wasserman et al., 2008). Instead, we

evidence that aged animals have greater axonal damage that extends further into the parenchyma surrounding the hematoma, supporting the hypothesis that factors emanating from the hematoma propagate the damage. White matter damage propagating into the parenchyma is especially interesting compared with the very limited neuron death outside the hematoma in either young or aged animals. Although our results do not support activated microglia/macrophages initiating the axonal damage, they might exacerbate it by transecting axons. Increased white matter injury in aged animals after ischemic stroke has been attributed to increased glutamate-mediated excitotoxicity (Baltan et al., 2008), which is also a possibility for ICH because glutamate is elevated around the hematoma (Qureshi et al., 2003). Alternatively, the increased edema seen in aged animals after ICH (Gong et al., 2004) might exacerbate axonal damage by allowing more blood proteins into the brain. Most importantly for potential therapeutic approaches, the delayed time course of white matter damage presents a reasonable therapeutic opportunity that should be targeted in future attempts to improve the neurological outcome after ICH.

Acknowledgments

Excellent technical assistance was provided by Helen Wang. JKW's work would not have been accomplished without support from Talea Coghlin. Supported by operating grants to LCS from the Heart & Stroke Foundation, Ontario Chapter (HSFO; T5546; T6279), and scholarships to JKW from the Peterborough KM Hunter Foundation, and the Heart & Stroke Foundation, Ontario Chapter.

References

Priorities for clinical research in intracerebral hemorrhage: report from a National Institute of Neurological Disorders and Stroke workshop, 2005. Stroke 36, e23–e41.

Badan, I., Dinca, I., Buchhold, B., Suofu, Y., Walker, L., Gratz, M., Platt, D., Kessler, C.H., Popa-Wagner, A., 2004. Accelerated accumulation of N- and C-terminal beta APP fragments and delayed recovery of microtubule-associated protein 1B expression following stroke in aged rats. Eur. J. Neurosci. 19, 2270–2280.

Baltan, S., Besancon, E.F., Mbow, B., Ye, Z., Hamner, M.A., Ransom, B.R., 2008. White matter vulnerability to ischemic injury increases with age because of enhanced excitotoxicity. J. Neurosci. 28, 1479–1489.

Broderick, J., Connolly, S., Feldmann, E., Hanley, D., Kase, C., Krieger, D., Mayberg, M., Morgenstern, L., Ogilvy, C.S., Vespa, P., Zuccarello, M., 2007. Guidelines for the management of spontaneous intracerebral hemorrhage in adults: 2007 update: a guideline from the American Heart Association/American Stroke Association Stroke Council, High Blood Pressure Research Council, and the Quality of Care and Outcomes in Research Interdisciplinary Working Group. Stroke 38, 2001–2023.

Coleman, M.P., Perry, V.H., 2002. Axon pathology in neurological disease: a neglected therapeutic target. Trends Neurosci. 25, 532–537.

Del Bigio, M.R., Yan, H.J., Buist, R., Peeling, J., 1996. Experimental intracerebral hemorrhage in rats. Magnetic resonance imaging and histopathological correlates. Stroke 27, 2312–2319.

Engel, S., Schluesener, H., Mittelbronn, M., Seid, K., Adjodah, D., Wehner, H.D., Meyermann, R., 2000. Dynamics of microglial activation after human traumatic brain injury are revealed by delayed expression of macrophage-related proteins MRP8 and MRP14. Acta Neuropathol. 100, 313–322.

Felberg, R.A., Grotta, J.C., Shirzadi, A.L., Strong, R., Narayana, P., Hill-Felberg, S.J., Aronowski, J., 2002. Cell death in experimental intracerebral hemorrhage: the "black hole" model of hemorrhagic damage. Ann. Neurol. 51, 517–524.

Fordyce, C.B., Jagasia, R., Zhu, X., Schlichter, L.C., 2005. Microglia Kv1.3 channels contribute to their ability to kill neurons. J. Neurosci. 25, 7139–7149.

Gentleman, S.M., Nash, M.J., Sweeting, C.J., Graham, D.I., Roberts, G.W., 1993. Beta-amyloid precursor protein (beta APP) as a marker for axonal injury after head injury. Neurosci. Lett. 160, 139–144.

Gong, C., Hoff, J.T., Keep, R.F., 2000. Acute inflammatory reaction following experimental intracerebral hemorrhage in rat. Brain Res. 871, 57–65.

Gong, Y., Hua, Y., Keep, R.F., Hoff, J.T., Xi, G., 2004. Intracerebral hemorrhage: effects of aging on brain edema and neurological deficits. Stroke 35, 2571–2575.

Huang, F.P., Xi, G., Keep, R.F., Hua, Y., Nemoianu, A., Hoff, J.T., 2002. Brain edema after experimental intracerebral hemorrhage: role of hemoglobin degradation products. J. Neurosurg. 96, 287–293.

Justicia, C., Panes, J., Sole, S., Cervera, A., Deulofeu, R., Chamorro, A., Planas, A.M., 2003. Neutrophil infiltration increases matrix metalloproteinase-9 in the ischemic brain after occlusion/reperfusion of the middle cerebral artery in rats. J. Cereb. Blood Flow Metab. 23, 1430–1440.

Kaushal, V., Koeberle, P.D., Wang, Y., Schlichter, L.C., 2007. The Ca2+-activated K+ channel KCNN4/KCa3.1 contributes to microglia activation and nitric oxide-dependent neurodegeneration. J. Neurosci. 27, 234–244.

Kaushal, V., Schlichter, L.C., 2008. Mechanisms of microglia-mediated neurotoxicity in a new model of the stroke penumbra. J. Neurosci. 28, 2221–2230.

Koo, E.H., Sisodia, S.S., Archer, D.R., Martin, L.J., Weidemann, A., Beyreuther, K., Fischer, P., Masters, C.L., Price, D.L., 1990. Precursor of amyloid protein in Alzheimer disease undergoes fast anterograde axonal transport. Proc. Natl. Acad. Sci. U S A 87, 1561–1565.

MacLellan, C.L., Auriat, A.M., McGie, S.C., Yan, R.H., Huynh, H.D., De Butte, M.F., Colbourne, F., 2006. Gauging recovery after hemorrhagic stroke in rats: implications for cytoprotection studies. J. Cereb. Blood Flow Metab. 26, 1031–1042.

MacLellan, C.L., Silasi, G., Poon, C.C., Edmundson, C.L., Buist, R., Peeling, J., Colbourne, F., 2008. Intracerebral hemorrhage models in rat: comparing collagenase to blood infusion. J. Cereb. Blood Flow Metab. 28, 516–525.

Marik, C., Felts, P.A., Bauer, J., Lassmann, H., Smith, K.J., 2007. Lesion genesis in a subset of patients with multiple sclerosis: a role for innate immunity? Brain 130, 2800–2815.

Matsuo, A., Lee, G.C., Terai, K., Takami, K., Hickey, W.F., McGeer, E.G., McGeer, P.L., 1997. Unmasking of an unusual myelin basic protein epitope during the process of myelin degeneration in humans: a potential mechanism for the generation of autoantigens. Am. J. Pathol. 150, 1253–1266.

Medana, I.M., Esiri, M.M., 2003. Axonal damage: a key predictor of outcome in human CNS diseases. Brain 126, 515–530.

Morioka, T., Kalehua, A.N., Streit, W.J., 1993. Characterization of microglial reaction after middle cerebral artery occlusion in rat brain. J. Comp. Neurol. 327, 123–132.

Neumann, H., 2003. Molecular mechanisms of axonal damage in inflammatory central nervous system diseases. Curr. Opin. Neurol. 16, 267–273.

Nguyen, H.X., O'Barr, T.J., Anderson, A.J., 2007. Polymorphonuclear leukocytes promote neurotoxicity through release of matrix metalloproteinases, reactive oxygen species, and TNF-alpha. J. Neurochem. 102, 900–912.

Otsuka, N., Tomonaga, M., Ikeda, K., 1991. Rapid appearance of beta-amyloid precursor protein immunoreactivity in damaged axons and reactive glial cells in rat brain following needle stab injury. Brain Res. 568, 335–338.

Popa-Wagner, A., Schroder, E., Walker, L.C., Kessler, C., 1998. beta-Amyloid precursor protein and ss-amyloid peptide immunoreactivity in the rat brain after middle cerebral artery occlusion: effect of age. Stroke 29, 2196–2202.

Qureshi, A.I., Ali, Z., Suri, M.F., Shuaib, A., Baker, G., Todd, K., Guterman, L.R., Hopkins, L.N., 2003. Extracellular glutamate and other amino acids in experimental intracerebral hemorrhage: an in vivo microdialysis study. Crit. Care Med. 31, 1482–1489.

Redford, E.J., Kapoor, R., Smith, K.J., 1997. Nitric oxide donors reversibly block axonal conduction: demyelinated axons are especially susceptible. Brain 120, 2149–2157.

Rincon, F., Mayer, S.A., 2004. Novel therapies for intracerebral hemorrhage. Curr. Opin. Crit. Care 10, 94–100.

Rosenberg, G.A., Mun-Bryce, S., Wesley, M., Kornfeld, M., 1990. Collagenase-induced intracerebral hemorrhage in rats. Stroke 21, 801–807.

Schmued, L.C., 1990. A rapid, sensitive histochemical stain for myelin in frozen brain sections. J. Histochem. Cytochem. 38, 717–720.

Sherriff, F.E., Bridges, L.R., Sivaloganathan, S., 1994. Early detection of axonal injury after human head trauma using immunocytochemistry for beta-amyloid precursor protein. Acta Neuropathol. 87, 55–62.

Stephenson, D.T., Rash, K., Clemens, J.A., 1992. Amyloid precursor protein accumulates in regions of neurodegeneration following focal cerebral ischemia in the rat. Brain Res. 593, 128–135.

Stone, J.R., Okonkwo, D.O., Dialo, A.O., Rubin, D.G., Mutlu, L.K., Povlishock, J.T., Helm, G.A., 2004. Impaired axonal transport and altered axolemmal permeability occur in distinct populations of damaged axons following traumatic brain injury. Exp. Neurol. 190, 59–69.

Streit, W.J., Walter, S.A., Pennell, N.A., 1999. Reactive microgliosis. Prog. Neurobiol. 57, 563–581.

Tepper, J.M., Abercrombie, E.D., Bolam, J.P., 2007. Basal ganglia macrocircuits. Prog. Brain Res. 160, 3–7.

Wagner, K.R., Dean, C., Beiler, S., Bryan, D.W., Packard, B.A., Smulian, A.G., Linke, M.J., de Court, 2005. Plasma infusions into porcine cerebral white matter induce early edema, oxidative stress, pro-inflammatory cytokine gene expression and DNA fragmentation: implications for white matter injury with increased blood-brain-barrier permeability. Curr. Neurovasc. Res. 2, 149–155.

Wang, J., Dore, S., 2007. Inflammation after intracerebral hemorrhage. J. Cereb. Blood Flow Metab. 27, 894–908.

Wasserman, J.K., Schlichter, L.C., 2007a. Neuron death and inflammation in a rat model of intracerebral hemorrhage: effects of delayed minocycline treatment. Brain Res. 1136, 208–218.

Wasserman, J.K., Schlichter, L.C., 2007b. Minocycline protects the blood-brain barrier and reduces edema following intracerebral hemorrhage in the rat. Exp. Neurol. 207, 227–237.

Wasserman, J.K., Yang, H., Schlichter, L.C., 2008. Glial responses, neuron death and lesion resolution after intracerebral hemorrhage in young versus aged rats. Eur. J. Neurosci. 28, 1316–1328.

Wasserman, J.K., Zhu, X., Schlichter, L.C., 2007. Evolution of the inflammatory response in the brain following intracerebral hemorrhage and effects of delayed minocycline treatment. Brain Res. 1180, 140–154.

Xi, G., Hua, Y., Keep, R.F., Younger, J.G., Hoff, J.T., 2001. Systemic complement depletion diminishes perihematomal brain edema in rats. Stroke 32, 162–167.

Yam, P.S., Takasago, T., Dewar, D., Graham, D.I., McCulloch, J., 1997. Amyloid precursor protein accumulates in white matter at the margin of a focal ischaemic lesion. Brain Res. 760, 150–157.